

$$\bar{\lambda} = \frac{L}{r_x} \cdot \frac{1}{\pi} \cdot \sqrt{\frac{\sigma_y}{E}} \quad (1)$$

$\bar{\lambda}$: Slenderness ratio parameter

L : Length (mm)

r_x : Radius of gyration over x axis (mm)

σ_y : Yield strength (MPa)

E : Young's modulus (MPa)

Table 1 Column specification (material: SUS316)

Cross sectional area	A	(mm ²)	2597
Length	L	(mm)	2600
Slenderness ratio parameter	$\bar{\lambda}$	-	0.861
Radius of gyration over x axis	r_x	(mm)	35.7
Yield strength	σ_y	(MPa)	251

Table 2 Gusset plate specification (material: SM400A)

Fixed point distance	a	(mm)	295
Thickness	t	(mm)	9
Yield strength	σ_y	(MPa)	293

Eq. 1¹⁾, governs the overall buckling behavior of the column, while the $a/(2t)$ ratio governs the local buckling behavior of the gusset plates.

Both parameters are determined by using the most frequently recorded values in existing bridges in Japan. In addition, as one of the objectives of this experiment is to observe the buckling behavior of the column, the slenderness ratio parameter was chosen with careful considerations so that the load carrying capacity of the column would be less than the load at which local buckling of the gusset plate and so that the bolt slippage does not occur. The specifications of the column and gusset plate are summarized in **Table 1** and **Table 2**.

For the cyclic compression loading, the axial compression test was conducted with repetitions of loading and unloading at various intervals. For the cyclic tension-compression loading, the specimen was loaded with similar repetitions but in both tension and compression. The reference points for the intervals were based on the calculated yield load, the experimental maximum load and the vertical displacement at the maximum load. Both the cyclic compression and cyclic tension-compression loading pattern includes three cycles of loading and unloading in various steps. The tensile region of the cyclic tension-compression loading was limited to avoid the slippage of the bolt, as shown in **Fig. 2**. Four displacement transducers were placed in the vertical direction to measure the average vertical

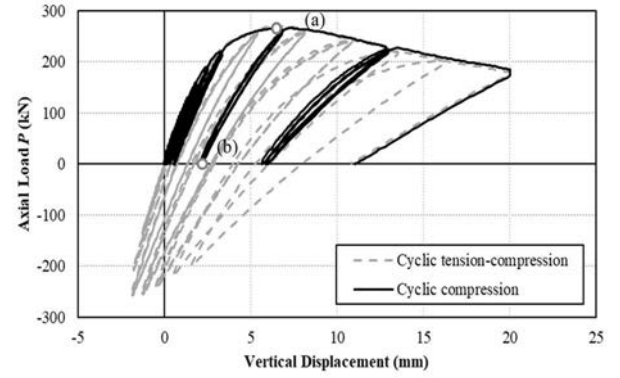


Fig. 2 Load-vertical displacement

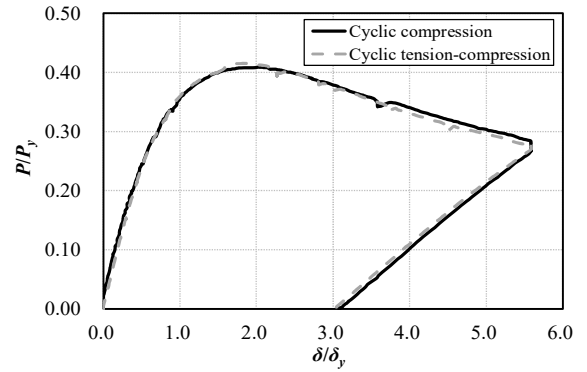


Fig. 3 Envelope load-vertical displacement

displacement, and horizontal displacement transducers were placed at three cross-sections along the length of the column to measure the column's out-of-plane deflection. Strain gauges were attached to the column and gusset plates, and clip-on gauges were attached at the end of the column to measure the bolt-connection slippage.

3. RESULTS AND DISCUSSIONS

The load-vertical displacement relationships for both loading types, as shown in **Fig. 2**, shows a maximum load of approximately 266 kN and 270 kN for the cyclic compression loading and cyclic tension-compression loading, respectively. Judging from the overall behavior of the curve, including the initial rigidity and the ductility of the column, it can be assumed that there is a negligible difference in the two results. In addition, the results in both loading patterns were also unaffected by the repeated loading and unloading during the three cycles. A similar result can be observed through the envelope curves, as shown in **Fig. 3**. With a similar maximum load and elastoplastic behavior, it can be concluded that the loading type in this experiment has negligible effect on the load carrying capacity and ductility.

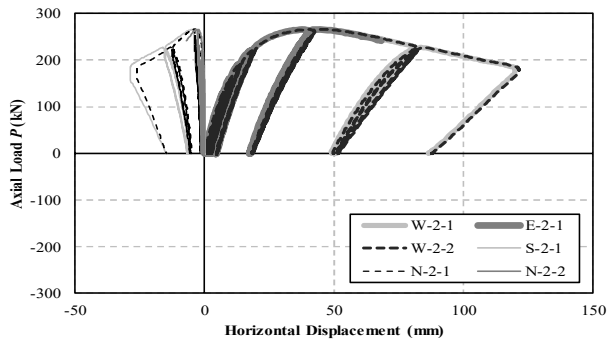


Fig. 4 Load-lateral displacement (cyclic compression)

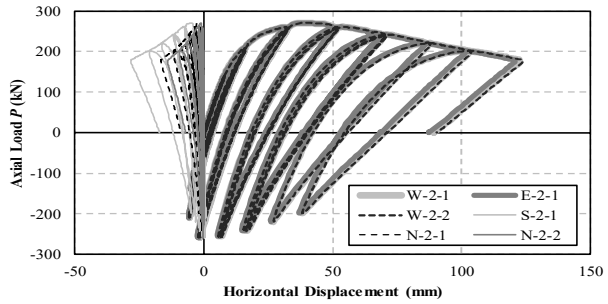


Fig. 5 Load-lateral displacement (cyclic tension-compression)

Fig. 4 shows the out-of-plane and in-plane deflection at the column's longitudinal center during cyclic compression loading. The reference points for each of the results as measured by the displacement transducers are shown in Fig. 1. It can be observed that the dominant deflection occurs over the strong axis, where displacement transducers W-2-1, W-2-2, and E-2-1 all show equal magnitudes of a large deflection. In comparison, the displacement transducers N-2-1, N-2-2, and S-2-1 show a relatively low magnitude of deflection. As shown in Fig. 5, a similar pattern was observed for the cyclic tension-compression loading where the maximum deflections are almost identical and the tendencies agree. Overall buckling was observed in the column for both cases, and neither local buckling in the gusset plates nor slippage in the bolt connections were observed. As shown in Fig. 6 for the cyclic compression loading, the strains on the gusset plates at the maximum load and at the point after unloading from the maximum load were compared. The reference points for (a) and (b) are shown in Fig. 2. The examined face of the gusset is the face that is connected to the column, as shown in Fig. 1. Although the maximum strain reaches roughly the yield strain of the gusset, relatively low magnitudes of residual strains were observed after the unloading from P_{max} . As the principle stress diagrams of the cyclic compression loading in Fig. 7 also shows, the magnitude and direction

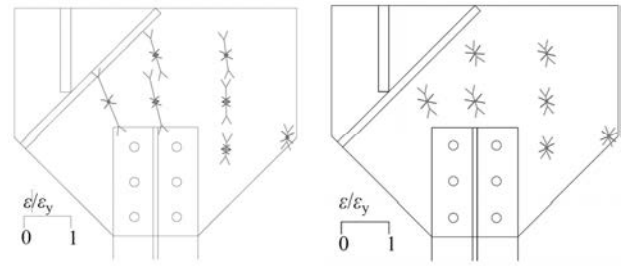


Fig. 6 Gusset principle stresses (cyclic compression)

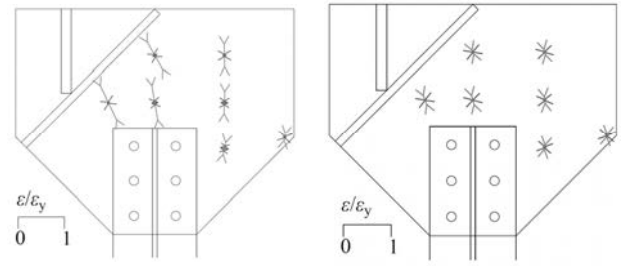


Fig. 7 Gusset principle stresses (cyclic tension-compression)

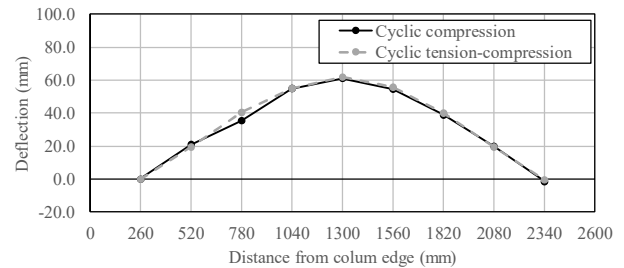


Fig. 8 Out-of-plane residual deflection

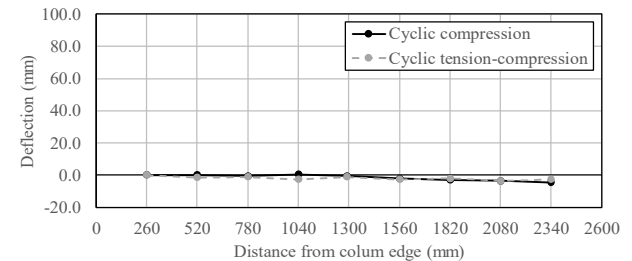


Fig. 9 In-plane residual deflection

of the principle stresses are in agreement with that of the cyclic compression loading. Therefore, it can be inferred that the loading pattern for this experiment between the cyclic compression and cyclic tension-compression loading has an insignificant effect on both the principles strains and the overall deflection of the column. In addition to the out-of-plane and in-plane deformations, the residual deformations in both directions were also examined. The results of the measurements for both the cyclic compression loading specimen and the cyclic tension compression loading specimen are shown in Fig. 8 and Fig. 9 in the out-of-plane and in-plane directions,

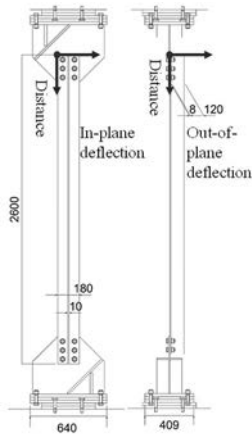


Fig. 10 Direction for residual deflections

respectively. The origin and directions of the measurements can be found in Fig. 10. Similar to the results of the out-of-plane and in-plane deflections, the major residual deformation is observed in the out-of-plane direction over the column's strong axis. This occurred due to the eccentricity between the column and the gusset plate where the direction of the eccentricity is perpendicular to the column's longitudinal direction and strong axis. However, the small discrepancy between the results for the cyclic compression loading and cyclic tension-compression loading show that the residual deformations in both directions seem to not be affected by the loading patterns compared in this experiment.

Lastly, the experimental results were compared with the ultimate strength curves specified in the "Specifications for Highway Bridges," where the ultimate strength curves for columns excluding welded box sections and that for angle sections and T sections considering eccentricity are shown in Eq. 2 and Eq. 3²⁾, respectively. The experimental results are plotted against the ultimate strength curves, as shown in Fig. 11. The experimental results being higher than the Eq. 3 shows that the design ultimate strength curve for angle sections and T sections considering eccentricity can safely be used to evaluate the ultimate strength of T section long columns made of stainless steel, regardless of the loading type as for the two test specimens.

$$\frac{\sigma_{cr}}{\sigma_y} = \begin{cases} 1.00 & (\bar{\lambda} \leq 0.2) \\ 1.109 - 0.545\bar{\lambda} & (0.2 < \bar{\lambda} \leq 1.0) \\ 1/(0.733 + \bar{\lambda}^2) & (1.0 < \bar{\lambda}) \end{cases} \quad (2)$$

$$\frac{\sigma_{cud}}{\sigma_y} = \frac{\sigma_{cr}}{\sigma_y} \left(0.5 + \frac{L/r_x}{1000} \right) \quad (3)$$

σ_{cr} : Buckling strength (MPa)

σ_{cud} : Buckling strength with eccentricity (MPa)

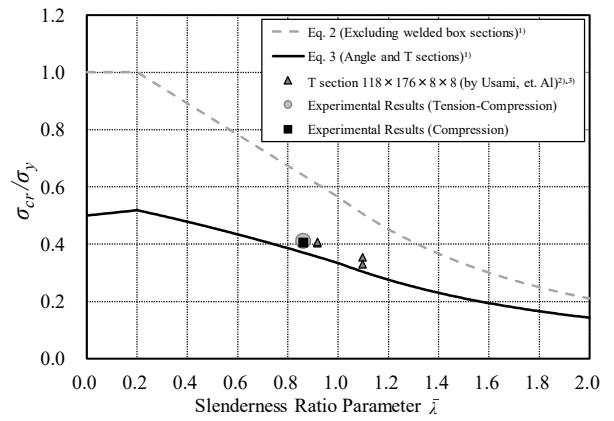


Fig. 11 Ultimate strength curve

4. CONCLUSIONS

In this experiment, the loading pattern had little effect on the load-vertical displacement relationship, load carrying capacity, and buckling mode. For both specimens, it is possible to evaluate the ultimate strength of the members based on previous studies with conventional steel.

ACKNOWLEDGEMENTS: This investigation was conducted as a joint research with Public Works Research Institute, universities, and organizations. The authors wish to express their deepest gratitude for their contributions, with a special thanks to Yui Iwasawa for contributing to the research results.

REFERENCES

- 1) Japan Road Association (2017), "Specifications for Highway Bridges, Part II; Steel Bridges", (in Japanese).
- 2) Usami, T. and Fukumoto, Y. (1972), "Compressive Strength and Design of Bracing Members with Angle or Tee Section", Journal of Japan Society of Civil Engineers, Vol.201, pp.43-50.
- 3) Usami, T. and Galambos, T. V. (1971), "Eccentrically Loaded Single-Angle Columns", Pub1. IABSE, Vol.31-II, pp.153-18